Nano Research
2019, 12(1): 19–23

ISSN 1998-0124 CN 11-5974/O4
https://doi.org/10.1007/s12274-018-2056-2

Research Article

Solution-processed highly adhesive graphene coatings for corrosion inhibition of metals

Gi-Cheol Son[1,§], Deuk-Kyu Hwang[3,§], Jaewon Jang[1], Sang-Soo Chee[1], Kyusang Cho[1], Jae-Min Myoung[3] (✉), and Moon-Ho Ham[1,2] (✉)

[1] *School of Materials Science and Engineering, Gwangju Institute of Science and Technology (GIST), 123 Cheomdangwagi-ro, Buk-gu, Gwangju 61005, Republic of Korea*
[2] *Research Institute for Solar and Sustainable Energies, Gwangju Institute of Science and Technology (GIST), 123 Cheomdangwagi-ro, Buk-gu, Gwangju 61005, Republic of Korea*
[3] *Department of Materials Science and Engineering, Yonsei University, 50 Yonsei-ro, Seodaemun-gu, Seoul 03722, Republic of Korea*
[§] *Gi-Cheol Son and Deuk-Kyu Hwang contributed equally to this work.*

Received: 4 January 2018 / **Revised:** 4 March 2018 / **Accepted:** 18 March 2018

ABSTRACT

The corrosion of metals can be induced by different environmental and operational conditions, and protecting metals from corrosion is a serious concern in many applications. The development of new materials and/or technologies to improve the efficiency of anti-corrosion coatings has attracted renewed interest. In this study, we develop a protective coating composed of a bilayer structure of reduced graphene oxide (RGO)/graphene oxide (GO) applied to Cu plates by spray-coating and subsequent annealing. The annealing of the GO/Cu plates at 120 °C produces a bilayer structure of RGO/GO by the partial reduction of the spray-coated GO layer. This induces superior corrosion resistance and adhesion strength compared to those of GO/Cu and RGO/Cu plates because of the hydrophobic nature of the RGO surface exposed to the surroundings and the formation of Cu–O bonds with the O-based functional groups of GO. This approach provides a viable and scalable route for using graphene coatings to protect metal surfaces from corrosion.

KEYWORDS

graphene, metal, surface coating, corrosion, solution process

1 Introduction

Metals and metal alloys are used extensively in electronics, automobiles, airplanes, and many other machines essential to modern life. In general, most metals are chemically unstable in the environment and corrode over time, especially when exposed to saline solutions like in the sea or coastal environments; corrosion degrades their structures and mechanical strengths. Preventing corrosion is a major challenge for the metallurgical community; the most popular method adopted is the application of protective coatings. Considerable efforts have been made to develop new anti-corrosive coating materials, including inert metal and polymer coatings [1–3]. However, the incorporation of these protective coatings often disrupts the physical properties and dimensional tolerances of the underlying metals because of the thickness of the coatings, which ranges from several to hundreds of micrometers. In addition, inert metal coatings are typically expensive and toxic [2], whereas polymer coatings suffer from poor adhesion to metal surfaces [3].

Since the first isolation of graphene, an atomically thin two-dimensional sheet of carbon atoms, by mechanical exfoliation from graphite in 2004, graphene has drawn significant interest for many applications, including electronics, catalysts, batteries, high-strength composites, and surface coatings [4–9]. This widespread interest mainly arises from the high electrical and thermal conductivity, optical transparency, large surface area, excellent mechanical strength and flexibility, remarkable chemical inertness, and complete impermeability of graphene. Recently, graphene has been considered as an alternative to conventional coating materials because of these advantages [6–9]. Ruoff et al. directly grew graphene films on Cu and Cu/Ni by chemical vapor deposition (CVD); the films were subsequently used as diffusion barriers against oxidation [7]. Furthermore, Bolotin et al. used graphene layers either directly grown by CVD or transferred onto Cu and Ni as protective coatings against corrosion [9]. The direct coating of graphene on target metals by CVD is limited because the target metal must be able to catalyze graphene growth [10]. The transferring of graphene causes damage to the graphene structure, such as tears and rips; transferred graphene also often shows poor adhesion [11, 12]. Compared to CVD, solution-based methods for applying graphene coatings are facile and cost-effective [13]. Recent studies have demonstrated that solution-processed graphene layers show good anti-corrosion performance, similar to that of CVD-grown graphene [8, 14]. To improve the corrosion and adhesion properties, Bohm et al. chemically bound graphene to metals through functionalization with 3-(aminopropyl)triethoxysilane (APTES) [8]. However, it is difficult to achieve uniform coatings of graphene layers via chemical functionalization with linkers over large areas.

In this study, graphene oxide (GO) sheets were deposited as an anti-corrosion protective coating on Cu plates by spray-coating, and then annealed to partially reduce the GO and to form Cu–O bonds by reacting the O-based functional groups of the remaining

Address correspondence to Jae-Min Myoung, jmmyoung@yonsei.ac.kr; Moon-Ho Ham, mhham@gist.ac.kr

GO sheets with Cu without the addition of linkers for chemical functionalization. Spray-coating is advantageous for fabricating large-area films with homogeneous spatial distributions over entire substrate surfaces using nanomaterials such as graphene [13], carbon nanotubes [15], and nanowires [16]. By controlling the annealing temperatures, highly structured reduced graphene oxide (RGO)/GO/Cu was created, which exhibited superior adhesion and anti-corrosion properties compared to GO/Cu and RGO/Cu plates.

2 Experimental

2.1 Preparation of GO sheets

GO sheets were prepared from graphite powder (~ 325 mesh, Alfa Aesar) using a modified Hummers method [17, 18]. Briefly, graphite powder was added slowly to a mixture of H_2SO_4 with $K_2S_2O_8$ and P_2O_5 for pre-oxidation. This mixture was reacted at 80 °C overnight and vacuum-filtered through a nylon filtration membrane. After drying at room temperature, the pre-oxidized graphite was dispersed and stirred in a H_2SO_4 solution in an ice bath. $KMnO_4$ was subsequently added slowly to the solution, and the resulting solution was reacted at 35 °C overnight for the complete oxidation of graphite. After adding deionized water and H_2O_2 to the solution, the resulting mixture was purified by rinsing several times with 10% HCl solution and deionized water, and then dialyzed against deionized water to remove the remaining impurities. Finally, the solution was dried at room temperature, producing GO sheets.

2.2 GO coating onto metal plates

For spray-coating, the GO films were dispersed in deionized water at the final concentration of 1 mg·mL^{-1} by bath sonication. Using this GO dispersion, homogeneous GO films were spray-coated onto 1 in × 1 in Cu plates that were heated to 70 °C on a hotplate, at the vertical distance of 15 cm. The film thickness was controlled by the amount of GO solution sprayed. To completely reduce the GO films coated on the metal plates, thermal treatments were performed at 150 °C for 6 h under a gas flow mixture of Ar/H_2. To enhance the adhesion between the GO or RGO film and the Cu surface, the GO- or RGO-coated metal plates were annealed at 90–120 °C for 1 h in air.

2.3 Corrosion and adhesion tests

Corrosion tests of the GO- and RGO-coated metal plates were performed by immersion in 5% aqueous NaCl solution at 35 °C for up to 96 h while monitoring for surface changes every 12 h. The adhesion between the GO or RGO and metal plates was evaluated by cross-cut tests. Using a knife and cutting guide, a lattice pattern with eleven cuts in each direction was made through the coating into the substrate at intervals of 1 mm. After applying and removing a standard adhesion tape (CT-24, Nichiban) over the lattice, the cut areas were inspected.

2.4 Characterization

The thicknesses of the films were measured by a surface profiler (DektakXT, Bruker). The surface morphologies of the films were analyzed by field-emission scanning electron microscopy (FESEM, JSM-7500F, JEOL). The presence of GO and RGO and the oxidation of the underlying metal plates were investigated using X-ray diffraction (XRD, D/Max-2500, Rigaku) with Cu Kα radiation (λ = 1.541 Å). The contact angles of water on the GO- or RGO-coated metal plates were measured using a contact angle analyzer (Phoenix-300, SEO). To investigate the interfacial states between the graphene layers and the underlying Cu, 10 nm-thick GO or RGO layers were spray-coated on the Cu plates. From these samples, the degree of reduction of the GO films and the oxidation degree of the underlying Cu plates were evaluated by X-ray photoelectron spectroscopy (XPS, K-Alpha, Thermo Scientific). The chemical bonding characteristics of the samples were analyzed using XPS as a function of etching depth. The presence and distributions of GO and RGO in the layers were investigated by high-resolution transmission electron microscopy (HRTEM, Technai G2 F30, FEI) with energy-dispersive X-ray spectroscopy (EDS).

3 Results and discussion

Figure 1(a) shows a schematic of the fabrication process of GO- or RGO-coated metal plates by spray-coating, which is a scalable technique for fabricating nanomaterial-based networked films. The GO solution with a concentration of 1 mg·mL^{-1}, prepared by a modified Hummers method, was spray-coated onto metal plates at the substrate temperature of 70 °C [17, 18]. The thicknesses of the GO films coated on the metal plates were linearly increased with the amount of GO solution used for spray coating (Fig. S1 in the Electronic Supplementary Material (ESM)). Although the surfaces of the Cu plates are rough, the FESEM images reveal that the GO films are uniformly deposited with thicknesses of 500 nm on the Cu plates by spray-coating (Figs. 1(b) and 1(c)). Therefore, this thickness was used; it is one to three orders of magnitude smaller than those of conventional metal or polymer coatings [1, 3]. These results demonstrate that spray-coating provides good uniformity and controllability of film thickness. When the GO films were reduced thermally, the thickness of the RGO films was decreased by approximately 20% because of the removal of O-containing functional groups from the graphene surface, inducing closer packing of the RGO laminates (Fig. S1 in the ESM) [19]. To enhance the adhesion between GO or RGO and the metal plates, annealing treatments were performed between 90 and 120 °C after coating with GO or RGO. At the annealing temperature of 120 °C, the color of the sample surface was slightly darker compared to that of the 90 °C-annealed GO/Cu plates, but was lighter than that of RGO/Cu plates, where GO was reduced to RGO at 150 °C (Fig. 2(a)). This indicates that higher annealing temperatures promote the reduction of GO [20].

The corrosion protection properties of the GO and RGO coatings on the metal plates were investigated by immersing the samples in a 5% salt solution (Fig. 2(a) and Fig. S2 in the ESM). The surfaces of the Cu and the as-coated GO/Cu plates show stains with a blue-green color after immersion for 12 and 36 h, respectively, indicating the oxidation of the Cu surfaces beneath the GO layers. The GO/Cu plate annealed at 90 °C exhibits similar corrosion behavior to the as-coated sample, while the sample surface remains unchanged even after immersion for 96 h for the GO/Cu plate annealed at 120 °C. Moreover, there is no visible change in the surface of the RGO-coated Cu plates after the corrosion tests. To identify the byproducts created on the sample surface, XRD measurements were performed (Fig. 2(b)). After immersion in the salt solution for 96 h, additional peaks are observed for the Cu, as-coated GO/Cu, and 90 °C-annealed GO/Cu plates in addition to

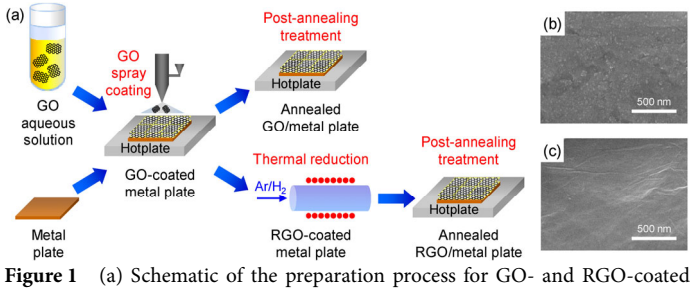

Figure 1 (a) Schematic of the preparation process for GO- and RGO-coated metal plates by spray-coating. FESEM images of (b) Cu and (c) as-coated GO/Cu plates.

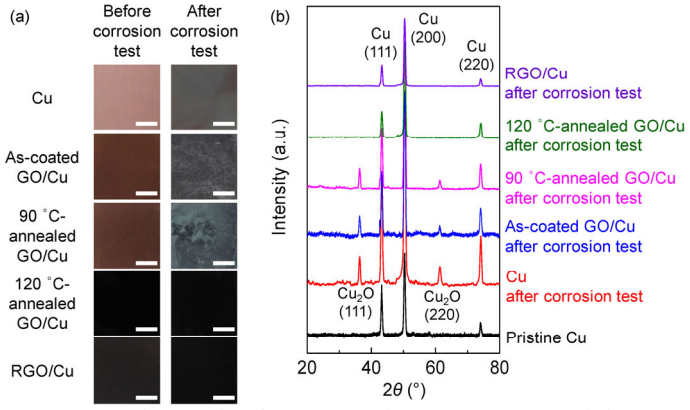

Figure 2 (a) Photographs of Cu, as-coated GO/Cu, 90 °C-annealed GO/Cu, 120 °C-annealed GO/Cu, and RGO/Cu plates before and after immersion in salt solutions for 96 h (scale bar: 5 mm). (b) XRD patterns of Cu, as-coated GO/Cu, 90 °C-annealed GO/Cu, 120 °C-annealed GO/Cu, and RGO/Cu plates after immersion in salt solutions for 96 h, together with the XRD pattern of the pristine Cu plate for comparison.

the peaks arising from Cu; the additional peaks correspond to the Cu_2O phase. This confirms the surface oxidation of the underlying Cu. In contrast, the 120 °C-annealed GO/Cu and RGO-coated Cu plates show only peaks arising from Cu. This demonstrates that the surface oxidation of the underlying metals is effectively prevented when the GO coating is annealed above 120 °C.

To further investigate the thermal annealing effects of the GO coatings of metal plates on corrosion protection performance, the water wettability of the graphene surfaces was determined by contact angle testing (Fig. 3). The water contact angle on the surface of the pristine Cu plate is 95°, indicating that the pristine Cu plate is hydrophobic. The surface becomes more hydrophilic upon GO coating because GO contains many O-related functional groups such as hydroxy, epoxy, and carboxyl groups [21]. When the GO/Cu plates are annealed at 90 °C, the water contact angle remains low (35°), comparable to that of the untreated GO/Cu plate (39°). This

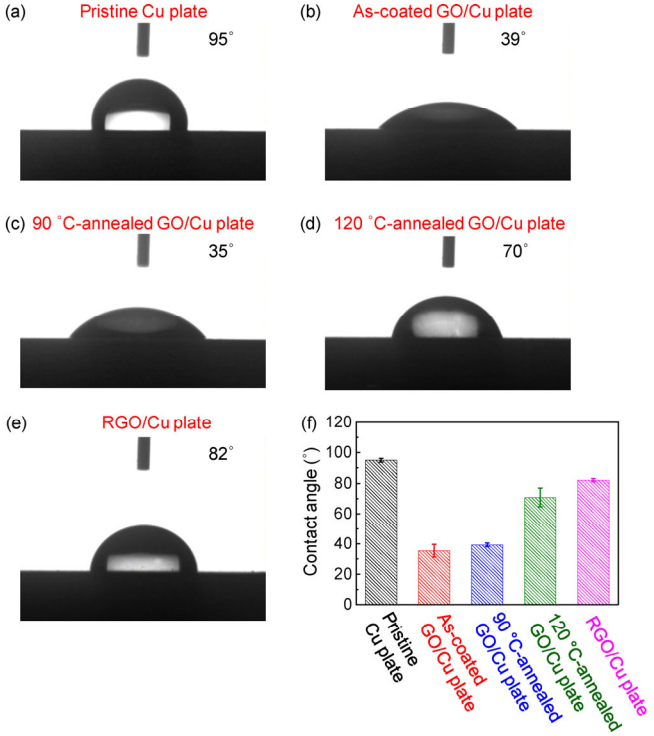

Figure 3 Water contact angles on the surfaces of (a) pristine Cu, (b) as-coated GO/Cu, (c) 90 °C-annealed GO/Cu, (d) 120 °C-annealed GO/Cu, and (e) RGO/Cu plates. (f) Comparison of water contact angles for all the samples.

indicates that thermal treatment at 90 °C does not change the surface characteristics of GO. However, with increasing annealing temperatures, the water contact angles are increased toward 90° and the sample surfaces become more hydrophobic because of the removal of O-related functional groups. These results demonstrate that the hydrophobic surfaces of 120 °C-annealed GO/Cu and RGO/Cu plates protect the Cu surface against the salt solution by repelling water molecules, yielding superior corrosion inhibition.

In addition to corrosion inhibition, it is also important to determine whether the coating that protects the metal surface is adhered properly to the substrate to which it is applied. Figure 4 shows cross-cut adhesion test results for the as-coated GO/Cu, 90 °C-annealed GO/Cu, 120 °C-annealed GO/Cu, RGO/Cu plates, and 120 °C-annealed RGO/Cu, evaluated according to American Society for Testing and Materials (ASTM) standards. For the as-coated GO/Cu, most of the GO coating is peeled away from the Cu surface during the adhesion test. This is indicative of poor adhesion due to physical contact between GO and Cu. After the annealing of the GO/Cu plates at 90 and 120 °C, the adhesion properties are greatly improved, with the adhesion strength of 4B (that means that small flakes of the coating are detached at intersections; less than 5% of the area is affected) according to ASTM standards. This is likely due to the interactions between the graphene sheets and Cu surface induced during the thermal treatments. This mechanical robustness enables the use of the graphene coating for the protection of metals against corrosion. However, regardless of annealing, the RGO/Cu plates show poor adhesion between RGO and Cu.

To characterize the interactions between the graphene sheets and Cu surface, the chemical states of the graphene sheets and underlying Cu were investigated for the samples with 10-nm-thick graphene layers by XPS (Fig. 5). In the C 1s spectra, peaks arising from O-related bonds (i.e., C–O, C=O, and C–OH) in the GO/Cu plates are decreased upon thermal treatment, and the RGO/Cu plate shows very weak peaks (Fig. 5(a)) [22, 23]. In the Cu 2p spectra, a Cu^{1+} peak appears when the samples are annealed at 90 and 120 °C, but the peak intensity is decreased for the RGO-coated metal plate (Fig. 5(b)) [22]. These results indicate the partial removal of O-containing functional groups from the graphene surface and the formation of Cu–O bonds at the interface between graphene and Cu during the thermal treatments. To further obtain depth-resolved information of the samples, XPS measurements for the samples with 500-nm-thick graphene layers were conducted with Ar^+ etching. For the as-coated GO/Cu plate, the peaks in the C 1s spectra and the atomic percent areas of the subpeaks ascribed to C–C/C=C and C–O/C=O/C–OH remain almost unchanged regardless of the etching depth (Fig. 5(c)) [22, 23]. On the other hand, for the 120 °C-annealed GO/Cu plate, the atomic percent areas of the subpeaks assigned to C–C/C=C are decreased from 75% to 67%, but those of the subpeaks related to C–O/C=O/C–OH are increased from 25% to 33% when approaching the interface between graphene and Cu. This indicates the surface reduction of the GO layer by the thermal treatments. In

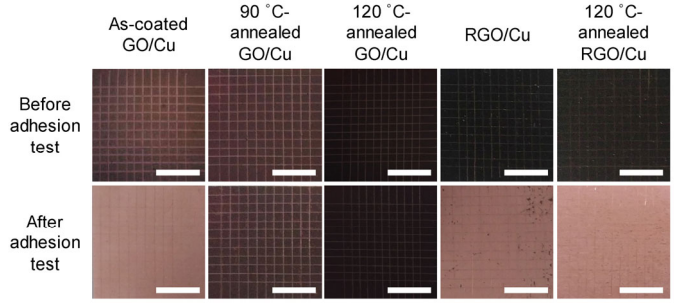

Figure 4 Photographs of as-coated GO/Cu, 90 °C-annealed GO/Cu, 120 °C-annealed GO/Cu, RGO/Cu, and 120 °C-annealed RGO/Cu plates before and after cross-cut tests (scale bar: 5 mm).

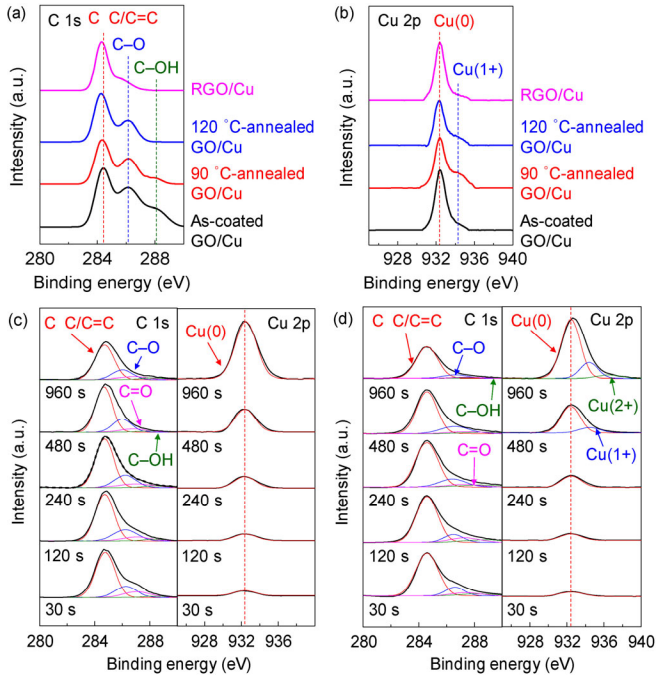

Figure 5 (a) C 1s and (b) Cu 2p XPS spectra of as-coated GO/Cu, 90 °C-annealed GO/Cu, 120 °C-annealed GO/Cu, and RGO/Cu plates. C 1s and Cu 2p XPS depth profile spectra of (c) as-coated and (d) 120 °C-annealed GO/Cu plates.

the depth profiles of the Cu 2p XPS spectra, a distinct peak appears near the interface between graphene and Cu for both as-coated and 120 °C-annealed GO/Cu plates [22]. However, the peak for the 120 °C-annealed sample is shifted to a higher binding energy than that of the as-coated sample, and is deconvoluted into two subpeaks corresponding to Cu^0 and Cu^{1+}. The appearance of the Cu^{1+} peak is most likely related to Cu–O bonds. Therefore, the improved adhesion strength for the 90 °C- and 120 °C-annealed GO/Cu plates is attributed to the formation of Cu–O bonds. Conversely, for the RGO-coated metal plates that were prepared by annealing at 150 °C, O-containing functional groups are removed completely, and no Cu–O bonds are formed, as no O-containing functional groups remained to interact with the Cu surface, resulting in poor adhesion properties.

The annealing treatments at 90 and 120 °C both induce outstanding adhesion performances for the resulting composites, but the corrosion resistance in salt solution for the 120 °C-annealed GO/Cu plates is significantly higher than that of the 90 °C-annealed GO/Cu plates. To further examine this phenomenon, we compared their water wettability and XPS spectra, both of which are useful for analyzing surface characteristics. For the 90 °C-annealed GO/Cu plate, the O-containing functional groups are only partially removed, and its surface remains hydrophilic. On the other hand, the 120 °C-annealed GO/Cu plate shows a more hydrophobic surface with fewer O-containing functional groups. Considering the corrosion and adhesion results, it is likely that in the graphene layer, the O-containing functional groups exposed to the surroundings are removed during the thermal treatment at 120 °C, causing the graphene surface to become hydrophobic while maintaining some O-containing functional groups within the graphene layers. Some of the remaining O-containing functional groups close to the Cu surface react to form Cu–O bonds, yielding a RGO/GO/Cu structure (Fig. 6). Another possibility for Cu–O bonds is the formation of Cu oxides on Cu by reacting O-containing functional groups and/or desorbed water molecules with Cu, without covalent bonds of RGO/GO and Cu. To address this possibility, the surface of a Cu plate was oxidized and GO was spray-coated onto the CuO_x/Cu. After

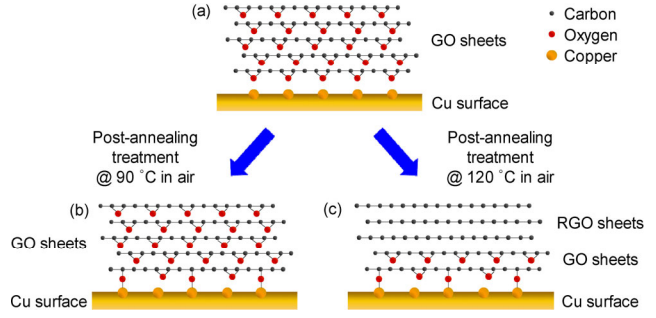

Figure 6 Schematics for the lamellar structures of graphene sheets coated on Cu plates, showing oxygen-based functional groups and Cu–O bonds formed upon post-annealing treatment: (a) as-coated GO/Cu, (b) 90 °C-annealed GO/Cu, and (c) 120 °C-annealed GO/Cu plates. The 120 °C-annealed GO/Cu plate creates a RGO/GO/Cu structure by partial reduction of the GO layer, leading to superior corrosion resistance and adhesion strength.

the annealing treatment, the GO/CuO_x/Cu plate showed poor adhesion (Fig. S3 in the ESM). This indicates that the formation of Cu–O bonds at the interface between graphene and Cu imparts robust adhesion for the samples. The removal of O-containing functional groups near the sample surface causes increased hydrophobicity of the graphene sheets, leading to the drastic improvement in corrosion resistance for the 120 °C-annealed sample. Shin et al. reported that ten layers of RGO were required to act as a diffusion barrier for gas, which strongly supports our finding that metals are protected by the surface reduction of the GO coating [14].

To further support the formation of this proposed structure, TEM and EDS analyses were performed (Fig. 7). The HRTEM images revealed that the GO exhibits an amorphous and disordered structure [24]. On the other hand, the RGO regions in the 120 °C -annealed GO/Cu and RGO/Cu plates show crystalline structures with the interplanar distance of 0.34 nm, which corresponded to the *d* spacing of graphene [24]. In the EDS profiles based on the elemental line-scanning mode, uniform C and O concentration distributions are observed for the as-coated GO/Cu, 90 °C-annealed GO/Cu, and RGO/Cu plates. However, for the 120 °C-annealed GO/Cu plate, the O concentration is gradually increased while the C concentration is decreased toward Cu surface, demonstrating the structure of RGO/GO formed by the partial reduction of the GO layer. This is consistent with the XPS depth profile results.

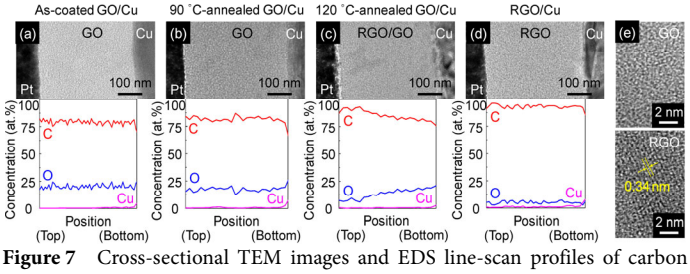

Figure 7 Cross-sectional TEM images and EDS line-scan profiles of carbon and oxygen in (a) as-coated GO/Cu, (b) 90 °C-annealed GO/Cu, (c) 120 °C-annealed GO/Cu, and (d) RGO/Cu plates. (e) Cross-sectional HRTEM images of GO and RGO regions.

4 Conclusions

In conclusion, we fabricated a RGO/GO bilayer structure on Cu metal plates by spray coating and subsequent annealing. This layer acted as an anti-corrosion coating, protecting the underlying metals from corrosion with excellent adhesion strength. The GO coating on the Cu plates did not protect the underlying Cu from corrosion despite its good adhesion, while the opposite behaviors were shown

for the RGO/Cu plates. The degree of reduction of the GO coated on the Cu plates was modulated by varying the annealing temperature, and the RGO/GO/Cu structure was successfully fabricated by annealing treatment at 120 °C. In this structure, the presence of RGO near the surface of the coating imparted a more hydrophobic surface, contributing to the improved corrosion resistance. Simultaneously, the GO adjacent to the Cu formed Cu–O bonds through the reaction of the O-containing functional groups with the Cu, resulting in improved adhesion strength. The process demonstrated in this study is an effective practical route for applying robust graphene coatings to protect metal surfaces, and has potential applications in various metal products.

Acknowledgements

This work was supported by the 2nd phase of the Fundamental R&D Programs for Core Technology of Materials funded by Ministry of Trade, Industry and Energy (MOTIE) (2015–2016), Future Semiconductor Device Technology Development Program (No. 10044868) funded by Ministry of Trade, Industry and Energy (MOTIE) and Korea Semiconductor Research Consortium (KSRC), Creative Materials Discovery Program through the National Research Foundation of Korea (NRF) funded by the Ministry of Science and ICT (No. 2017M3D1A1040828), Nano·Material Technology Development Program through the National Research Foundation of Korea(NRF) funded by Ministry of Science and ICT (No. 2017M3A7B4052798), Basic Science Research Program through the National Research Foundation of Korea (NRF) funded by the Ministry of Education (No. 2015R1D1A1A01058982), and GIST Research Institute (GRI) grant funded by the GIST.

Electronic Supplementary Material: Supplementary material (thickness of GO and RGO layers coated on Cu plates, photographs of Cu, as-coated GO/Cu, 90 °C-annealed GO/Cu, 120 °C-annealed GO/Cu, and RGO/Cu plates before and after corrosion tests, and photographs of 90 °C-annealed GO/CuO_x/Cu plate before and after cross-cut tests) is available in the online version of this article at https://doi.org/10.1007/s12274-018-2056-2.

References

[1] Gray, J. E.; Luan, B. Protective coatings on magnesium and its alloys—A critical review. *J. Alloy. Compd.* **2002**, *336*, 88–113.

[2] Tallman, D. E.; Spinks, G.; Dominis, A.; Wallace, G. G. Electroactive conducting polymers for corrosion control. *J. Solid State Electrochem.* **2002**, *6*, 73–84.

[3] Araujo, W. S.; Margarit, I. C. P.; Ferreira, M.; Mattos, O. R.; Neto, P. L. Undoped polyaniline anticorrosive properties. *Electrochim. Acta* **2001**, *46*, 1307–1312.

[4] Novoselov, K. S.; Geim, A. K.; Morozov, S. V.; Jiang, D.; Zhang, Y.; Dubonos, S. V.; Grigorieva, I. V.; Firsov, A. A. Electric field effect in atomically thin carbon films. *Science* **2004**, *306*, 666–669.

[5] Novoselov, K. S.; Fal'ko, V. I.; Colombo, L.; Gellert, P. R.; Schwab, M. G.; Kim, K. A roadmap for graphene. *Nature* **2012**, *490*, 192–200.

[6] Vadukumpully, S.; Paul, J.; Mahanta, N.; Valiyaveettil, S. Flexible conductive graphene/poly(vinyl chloride) composite thin films with high mechanical strength and thermal stability. *Carbon* **2011**, *49*, 198–205.

[7] Chen, S. S.; Brown, L.; Levendorf, M.; Cai, W. W.; Ju, S.-Y.; Edgeworth, J.; Li, X. S.; Magnuson, C. W.; Velamakanni, A.; Piner, R. D. et al. Oxidation resistance of graphene-coated Cu and Cu/Ni alloy. *ACS Nano* **2011**, *5*, 1321–1327.

[8] Aneja, K. S.; Bohm, S.; Khanna, A. S.; Bohm, H. L. M. Graphene based anticorrosive coatings for Cr(VI) replacement. *Nanoscale* **2015**, *7*, 17879–17888.

[9] Prasai, D.; Tuberquia, J. C.; Harl, R. R.; Jennings, G. K.; Bolotin, K. I. Graphene: Corrosion-inhibiting coating. *ACS Nano* **2012**, *6*, 1102–1108.

[10] Brownson, D. A. C.; Banks, C. E. The electrochemistry of CVD graphene: Progress and prospects. *Phys. Chem. Chem. Phys.* **2012**, *14*, 8264–8281.

[11] Kim, K.; Artyukhov, V. I.; Regan, W.; Liu, Y. Y.; Crommie, M. F.; Yakobson, B. I.; Zettl, A. Ripping graphene: Preferred directions. *Nano Lett.* **2012**, *12*, 293–297.

[12] Lin, Y.-M.; Valdes-Garcia, A.; Han, S.-J.; Farmer, D. B.; Meric, I.; Sun, Y.; Wu, Y.; Dimitrakopoulos, C.; Grill, A.; Avouris, P. et al. Wafer-scale graphene integrated circuit. *Science* **2011**, *332*, 1294–1297.

[13] Li, D.; Müller, M. B.; Gilje, S.; Kaner, R. B.; Wallace, G. G. Processable aqueous dispersions of graphene nanosheets. *Nat. Nanotechnol.* **2008**, *3*, 101–105.

[14] Kang, D.; Kwon, J. Y.; Cho, H.; Sim, J.-H.; Hwang, H. S.; Kim, C. S.; Kim, Y. J.; Ruoff, R. S.; Shin, H. S. Oxidation resistance of iron and copper foils coated with reduced graphene oxide multilayers. *ACS Nano* **2012**, *6*, 7763–7769.

[15] Lipomi, D. J.; Vosgueritchian, M.; Tee, B. C.-K.; Hellstrom, S. L.; Lee, J. A.; Fox, C. H.; Bao, Z. Skin-like pressure and strain sensors based on transparent elastic films of carbon nanotubes. *Nat. Nanotechnol.* **2011**, *6*, 788–792.

[16] Krantz, J.; Stubhan, T.; Richter, M.; Spallek, S.; Litzov, I.; Matt, G. J.; Spiecker, E.; Brabec, C. J. Spray-coated silver nanowires as top electrode layer in semitransparent P3HT: PCBM-based organic solar cell devices. *Adv. Funct. Mater.* **2013**, *23*, 1711–1717.

[17] Hummers, W. S., Jr.; Offeman, R. E. Preparation of graphitic oxide. *J. Am. Chem. Soc.* **1958**, *80*, 1339.

[18] Jang, K.; Hwang, D.-K.; Auxilia, F. M.; Jang, J.; Song, H.; Oh, B.-Y.; Kim, Y.; Nam, J.; Park, J.-W.; Jeong, S. et al. Sub-10-nm Co_3O_4 nanoparticles/graphene composites as high-performance anodes for lithium storage. *Chem. Eng. J.* **2017**, *309*, 15–21.

[19] Pei, S. F.; Zhao, J. P.; Du, J. H.; Ren, W. C.; Cheng, H.-M. Direct reduction of graphene oxide films into highly conductive and flexible graphene films by hydrohalic acids. *Carbon* **2010**, *48*, 4466–4474.

[20] Mattevi, C.; Eda, G.; Agnoli, S.; Miller, S.; Mkhoyan, K. A.; Celik, O.; Mastrogiovanni, D.; Granozzi, G.; Garfunkel, E.; Chhowalla, M. Evolution of electrical, chemical, and structural properties of transparent and conducting chemically derived graphene thin films. *Adv. Funct. Mater.* **2009**, *19*, 2577–2583.

[21] Gilje, S.; Han, S.; Wang, M. S.; Wang, K. L.; Kaner, R. B. A chemical route to graphene for device applications. *Nano Lett.* **2007**, *7*, 3394–3398.

[22] Lin, L. X.; Wu, H. P.; Green, S. J.; Crompton, J.; Zhang, S. W.; Horsell, D. W. Formation of tunable graphene oxide coating with high adhesion. *Phys. Chem. Chem. Phys.* **2016**, *18*, 5086–5090.

[23] Khusnun, N. F.; Jalil, A. A.; Triwahyono, S.; Jusoh, N. W. C.; Johari, A.; Kidam, K. Interaction between copper and carbon nanotubes triggers their mutual role in the enhanced photodegradation of p-chloroaniline. *Phys. Chem. Chem. Phys.* **2016**, *18*, 12323–12331.

[24] Wang, G. X.; Yang, J.; Park, J.; Gou, X. L.; Wang, B.; Liu, H.; Yao, J. Facile synthesis and characterization of graphene nanosheets. *J. Phys. Chem. C* **2008**, *112*, 8192– 8195.